Materials Research Proceedings 35 (2023) 182-190 https://doi.org/10.21741/9781644902714-22

Process parameters optimization in fused deposition modeling of polyether ether ketone

Emanuele Vaglio[1,2,a *], Erica Billè[2,b], Marina Franulović[3,c], Alessandro Gambitta[4,d], David Liović[3,e], Alfredo Rondinella[1,f], Marco Sortino[1,g], Giovanni Totis[1,h]

[1]Polytechnic Department of Engineering and Architecture, University of Udine, Via delle Scienze 206, 33100 Udine, Italy

[2]Department of Engineering and Architecture, University of Trieste, Via Alfonso Valerio 6/1, 34127 Trieste, Italy

[3]Faculty of Engineering, University of Rijeka, Vukovarska 58, 51000 Rijeka, Croatia

[4]Elettra-Sincrotrone Trieste, Area Science Park, 34149 Basovizza, Trieste, Italy

[a] emanuele.vaglio@uniud.it, [b] erica.bille@studenti.units.it, [c] marina.franulovic@riteh.hr, [d] alessandro.gambitta@elettra.eu, [e] dliovic@riteh.hr, [f] alfredo.rondinella@uniud.it, [g] marco.sortino@uniud.it, [h] giovanni.totis@uniud.it

Keywords: Additive Manufacturing, Material Extrusion, Process Parameters Optimization

Abstract. Fused Deposition Modeling is increasingly used for producing high-performing, creep-resistant, biocompatible, fireproof, highly-stable parts from polyether ether ketone. However, the knowledge on this process is still poor and fragmented, and the lack of relevant data inhibits many applications. In this paper, the effects of the nozzle temperature, nozzle speed and layer thickness on the properties of PEEK processed by Fused Deposition Modeling were investigated by performing indentation, tensile, Scanning Electron Microscope, Computer Tomography and Energy Dispersive X-ray Spectroscopy tests on as-built samples. The outgassing behavior was also analyzed, while the synchrotron radiation was used to characterize the structure of selected samples on a hitherto unexplored scale. The samples morphology was finally used to identify the optimal process window. The results provided new insights on the process and novel data enabling new applications.

Introduction

Polyether ether ketone (PEEK) is a semi-crystalline thermoplastic polymer belonging to the polyaryl ether ketone (PAEK) family. This fully recyclable material has excellent mechanical properties, chemical and radiation stability, biocompatibility and can withstand exceptionally high temperatures [1]. These unique properties make PEEK a highly appropriate material for multiple high-performance applications in several fields, including medical, aerospace, electrical, and chemical [2]. However, the processability of materials through additive techniques is today a fundamental requirement in these fields.

For a long time, Selective Laser Sintering (SLS) was the prevailing method used for additive processing of PEEK due to its high melting temperature. However, this approach has important drawbacks [3] that led scientists and industry to explore alternative solutions, such as Fused Deposition Modeling (FDM). Recently, Ding et al. [3] showed that increasing nozzle temperature (T_n) improves strength of PEEK parts produced by FDM due to decreased porosity and enhanced layer bonding. Sikder et al. [4] showed that heating the build chamber also improve the mechanical properties of the material, while heating the build platform enhances the adhesion of the material to the build surface but does not positively affect its mechanical properties. In the same study, it

Materials Research Proceedings 35 (2023) 182-190 https://doi.org/10.21741/9781644902714-22

was found that higher nozzle speed (v_n) and lower layer thickness (t_l) results in improved mechanical properties. Wu et al. [5] surprisingly observed that the best mechanical properties are obtained at intermediate values of t_l, and that also the raster angle has a significant effect on the tensile, compression, and three-point bending behavior. Vaezi et al. [6] proved that using a heated build platform and heated build chamber together can effectively mitigate the effects of the exceptional thermal stresses caused by the high melting temperature of PEEK and prevent the material's deformation and delamination. The authors noted that too high T_n results in low accuracy due to the extruded bead deformation and in material degradation, while too low T_n causes delamination due to insufficient bonding with the previous layers and nozzle clogging. Lee et al. [7] found that many factors influence the cooling rate and, in turn, crystallinity, including the build platform and build chamber temperature, v_n, the raster angle, and the number and geometry of parts produced simultaneously, which impact the time interval between successive layers. Yang et al. [8] showed that T_n influences multiple phenomena, including crystal melting, crystallization, bonding between extruded beads, and polymer degradation. The authors pointed out that performing thermal treatments may be the most effective way to improve the crystallinity and the mechanical properties of PEEK processed by FDM. El Magri et al. [9] found that the annealing temperature significantly influences the crystallization processes and that the treated material is stronger but less ductile. Zhao et al. [10] showed that none of the FDM parameters influence the chemical composition of the material.

Although noteworthy advancements in optimizing the FDM technology for processing PEEK have been made in recent years, the knowledge in this field remains scattered and incomplete. Therefore, further progress is needed to apply this technology in both conventional and advanced sectors that would benefit the most from its potential. In this paper, the effects of T_n, v_n, and t_l on the properties of parts produced from PEEK by FDM were analyzed to identify the optimal process condition and demonstrate the suitability of the process for critical applications.

Materials and methods

The samples tested in this work were prepared using a commercial PEEK filament of 1.75 mm diameter. Before use, the filament was analyzed by X-ray Computed Microtomography (X-ray μCT) and by Scanning Electron Microscope (SEM). No defects, impurities or pores were observed.

Subsequently, 18 cubic samples 20x20x20 mm in size were produced on an Intamsys Funmat HT machine. The cubes consisted of a core and a contour volume that overlapped with each other by 0.25 mm, and were produced one at a time by varying the process parameters according to a full factorial design of experiments. In more details, the nozzle temperature (T_n) was varied on 3 levels from 380 °C to 420 °C by discrete increments of 20 °C, the core nozzle speed (v_{nb}) was varied on 3 levels from 15 mm/s to 65 mm/s by increments of 25 mm/s, and the layer thickness (t_l) was varied on 2 levels corresponding to 0.1 mm and 0.2 mm. The core infill ratio was 100 % and it was obtained by depositing the material according to a bi-directional and rotated pattern resulting in a ±45 ° raster angle. The v_{nb} was reduced by 20 % during the deposition of the 6 top and bottom layers, according to the recommendations of the machine manufacturer. The contour was obtained instead by depositing 3 perimeter outlines at a reduced nozzle speed v_{nc}=0.5v_{nb}. In this way, real operating conditions were reproduced, which is crucial for optimizing the FDM process parameters for real applications. The nozzle diameter was kept fixed and equal to d_n=0.4 mm, while the building plate temperature and the building chamber temperature were T_{bp}=145 °C and T_{bc}=90 °C, respectively. The fan speed was set at 50 % of the maximum value admitted by the machine.

The so obtained samples were measured with a Mitutoyo ABS AOS digital caliper to assess the dimensional conformity, and they were analyzed with a Sensofar S neox confocal microscope to study the average surface roughness (R_a). The roughness profiles were extracted perpendicular to the grooves formed between layers or beads, and a cut-off wavelength of 0.8 mm was used for computing R_a. The top horizontal surfaces of the samples were also examined with a Zeiss Evo 40

Scanning Electron Microscope to characterize the defects caused by different process conditions and to analyze the chemical composition of the material by Energy Dispersive X-ray Spectroscopy (EDXS).

The samples produced using the extreme process configurations of the experimental design, representing the most and least favorable condition for obtaining fully dense parts, underwent X-ray μCT at the TomoLab station of Elettra Sincrotrone Trieste research center to investigate internal porosity. The voltage of the X-ray tube was set to 70 kV, and a 0.25 mm thick aluminum filter was positioned between the source and the samples. The system resolution was 18 μm. The porosities of the samples produced at high T_n were further analyzed on a resolution scale of 0.88 μm by using the SYRMEP Synchrotron X-ray μCT of Elettra Sincrotrone Trieste research center. The samples were subsequently sectioned and polished to obtain flat surfaces for hardness testing, which were performed according to the EN ISO 2039-1 standard with an applied load of 358 N. In details, 10 measurements were taken for each sample using a DuraJet G5 tester equipped with a 5 mm diameter spherical indenter. Eventually, 5 tensile test samples complying to the ISO 527-5A specimen type were produced using each set of the selected process parameters and tested using the strain rate of 1% min^{-1}, as recommended in ISO 521-1. The load cell of 25 kN was used for load measurements, while the Epsilontech 3442-010M-050M-ST extensometer with the gauge length of 20 mm was used for strain measurements during the tensile tests.

The Ultra-High Vacuum (UHV) behavior of the most promising sample was also evaluated by Residual Gas Analysis (RGA) performed using a mass spectrometer HAL 201 RC after bake-out at 120 °C and 200 °C.

Results and discussion

Dimensional conformity. Fig. 1 shows that the dimensional error parallel to the building plane increased with increasing T_n and t_l while decreasing v_n. Perpendicular to the building plane, the dimensional error was instead primarily influenced by T_n which again led to larger dimensional error by causing the extrusion of expanded and overly fluidized material that was spread out around the nozzle sides forming surface defects. Nevertheless, a weak non-monotonic effect of v_n was also observed. Interestingly, t_l did not affect the dimensional error in the vertical direction. The analysis of variance confirmed the significance of all the factors analyzed, except for t_l in relation to the dimensional error in the vertical direction.

Surface roughness. Major adverse effects on the quality of both horizontal and vertical surfaces were observed with increasing t_l, while minor favorable effects resulted from increasing v_n, presumably because the cooling efficiency was higher when the hot nozzle rapidly leaved the solidification area. No clear trends were observed for T_n. Instead, a sharp increase in R_a of horizontal surfaces due to the formation of visible defects was noticed above a specific threshold temperature. The analysis of variance confirmed the statistical validity of these findings.

Surface defects. The SEM inspections revealed that the horizontal surfaces of the samples produced at high T_n and low v_n (Fig. 2 (a)) exhibit burrs caused by over-extrusion (low speed) of expanded and overly fluidized (high temperature) material that is subsequently spread out by the nozzle. The severity of this flaw increased with increasing t_l due to a higher extrusion rate, and decreased with increasing v_n. However, it remained partially visible even in the samples produced at intermediate v_n. The horizontal surfaces of the samples produced at low T_n and high v_n (Fig. 2 (b)) exhibit instead lack of fusion voids between the deposited beads, and small elongated craters aligned in the direction of nozzle motion on their surface. These craters were likely a consequence of the high viscosity of the material, which reduces wettability [11] and promotes the formation of tears in the extruded and stretched material. It was found that craters and voids decreased both in number and size with increasing t_l and decreasing v_n. However, significant reductions in v_n are required to avoid this flaw since it was observed even in samples produced at intermediate v_n. The

Materials Research Proceedings 35 (2023) 182-190 https://doi.org/10.21741/9781644902714-22

horizontal surfaces of the samples produced at low T_n and low v_n (Fig. 2 (c)) finally appeared to be uniform and flawless, especially when thin layers were processed.

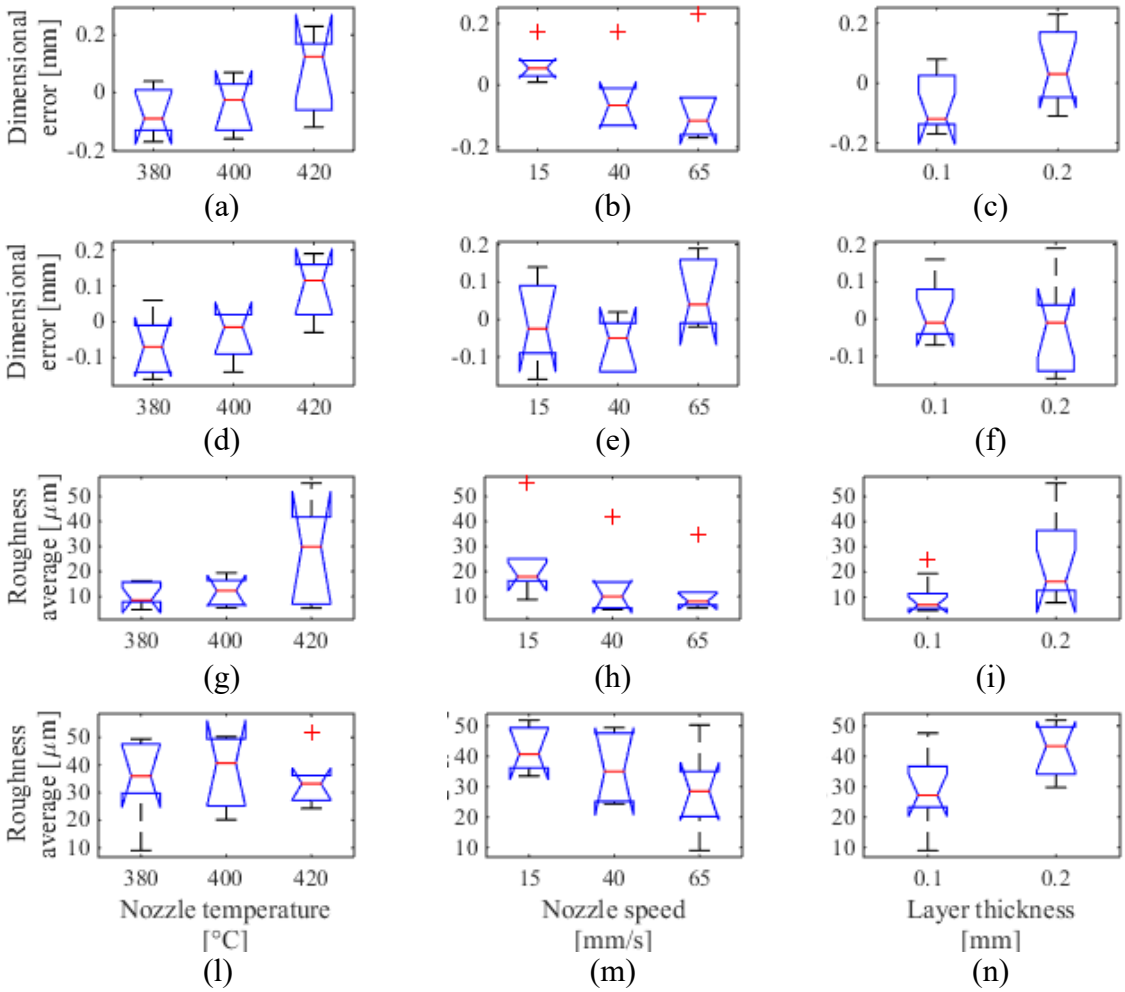

Fig. 1: Effect of the process parameters on (a), (b), (c) the dimensional error parallel to the building plane, (d), (e), (f) the dimensional error perpendicular to the building plane, (g), (h), (i) the roughness average of the surface parallel to the building plane and (l), (m), (n) the surface roughness of the surfaces perpendicular to the building plane.

Density. The samples produced at high v_n and high t_l were found to be exceedingly porous. Under low T_n condition (Fig. 3 (e)) the pores were formed due to under-extrusion, which resulted in air gaps between the deposited beads. Nevertheless, some spherical pores within the beads were also observed. Under high T_n condition (Fig. 3 (b)) the pores were instead uniformly distributed and had a rounded shape suggesting the entrapment of gas. This type of porosity is shown in more detail in Fig. 3 (f) where a complex structure of morphologically regular pores belonging to a wide dimensional spectrum reaching the nanoscale can be observed. The origin of these pores is still not clear. They are usually attributed to melt flow and solidification phenomena, or to gas voids primarily generated during the filament fabrication [12]. However, the preliminary tests performed on the filament used in this study proved the absence of pores.

The samples produced at low v_n and low t_l exhibited considerably higher density ρ. Under low T_n condition (Fig. 3 (d)), the initial layers of the sample were free of pores, while the upper layers contained a non-negligible amount of under-extrusion pores located between the deposited beads. This effect was attributed to the heated platform, which contributes to the energy input in the initial stages of the process and is crucial for interpreting the results of mechanical tests carried out on

Materials Research Proceedings 35 (2023) 182-190 https://doi.org/10.21741/9781644902714-22

thin tensile samples. Under high T_n condition (Fig. 3 (a)), the sample was instead practically free of pores, although the Synchrotron X-ray μCT revealed the presence of some isolated defects (Fig. 3 (c)).

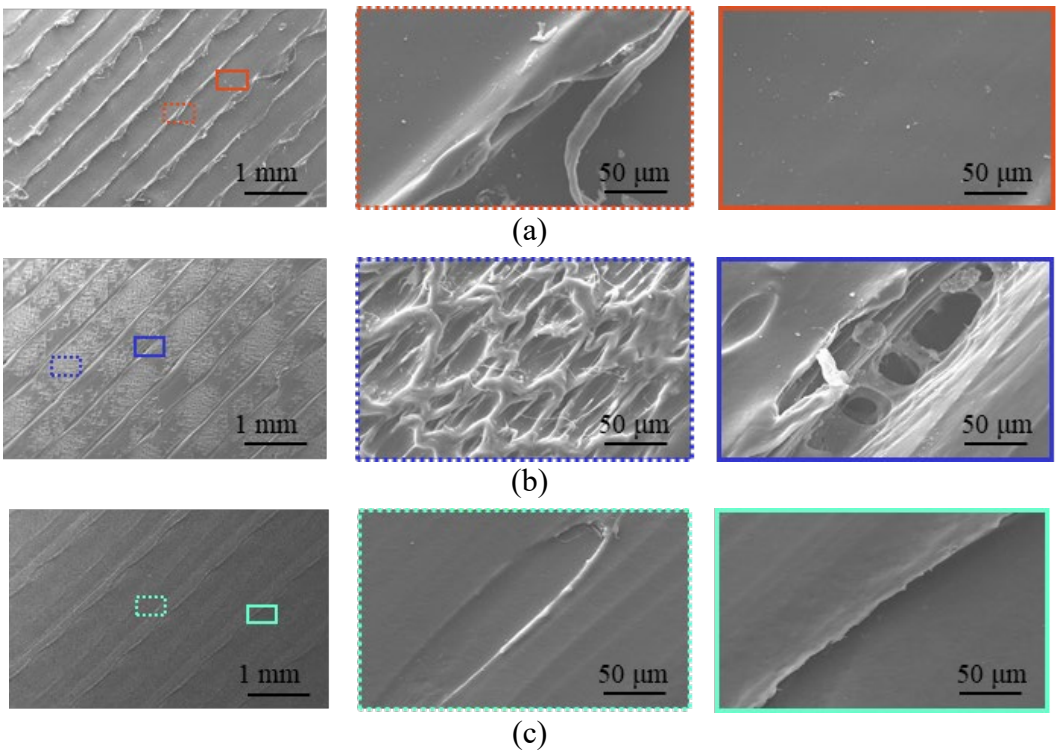

Fig. 2: SEM view of defects on the horizontal surfaces of the samples produced at (a) T_n=420 °C, v_{nb}=15 mm/s and t_l=0.1 mm, (b) T_n=380 °C, v_{nb}=65 mm/s and t_l=0.1 mm, (c) T_n=380 °C, v_{nb}=15 mm/s and t_l=0.1 mm.

Finally, no pores were found in the samples contour, except when the sample produced at high T_n, high v_n and high t_l was examined. Under these conditions, several under-extrusion defects formed in limited areas. However, these defects were attributed to casual factors since pores were localized and not detected in the sample produced at a lower T_n. Some isolated pores caused by insufficient interpenetration between core and contour were detected in all the samples.

Hardness. The mean and standard deviation of the hardness measured on the selected samples are reported in Table 1. Regardless of T_n, the combination of high v_n and high t_l resulted in very low hardness, while the combination of low v_n and low t_l resulted in better outcomes. Overall, a robust correlation with the internal porosity of the material was observed. It is worth noting that the hardness measured on the fully dense sample was slightly lower than the hardness of the conventionally processed PEEK.

Mechanical properties. The mechanical properties on the selected samples are reported in the Table 1. The lowest mean value of ultimate tensile strength (UTS) were obtained from the samples produced at low T_n, high v_n, and high t_l, which were also characterized by the lowest maximum elongation. Conversely, the highest mean value of the maximum elongation was found on samples produced at high T_n, low v_n, and low t_l. The mean values of the Young's modulus (E) were similar and within the statistical uncertainty. These results are in accordance with the density results shown in Fig. 3. However, it was not possible to establish a direct correlation between them since a large portion of the tensile samples consisted of contours, and the entire volume was deposited in close proximity to the building platform.

Materials Research Proceedings 35 (2023) 182-190 https://doi.org/10.21741/9781644902714-22

Table 1: Hardness and tensile test results given as mean value (standard deviation).

T_n [°C]	v_n [mm/s]	t_l [mm]	HB [MPa]	UTS [MPa]	E [MPa]	Max. elong. [%]
420	15	0.1	166 (20)	84 (3)	3161 (359)	126 (54)
380	15	0.1	147 (13)	83 (3)	3284 (277)	27 (8)
420	65	0.2	53 (4)	83 (1)	3267 (105)	17 (2)
380	65	0.2	53 (15)	77 (1)	3221 (272)	5 (1)

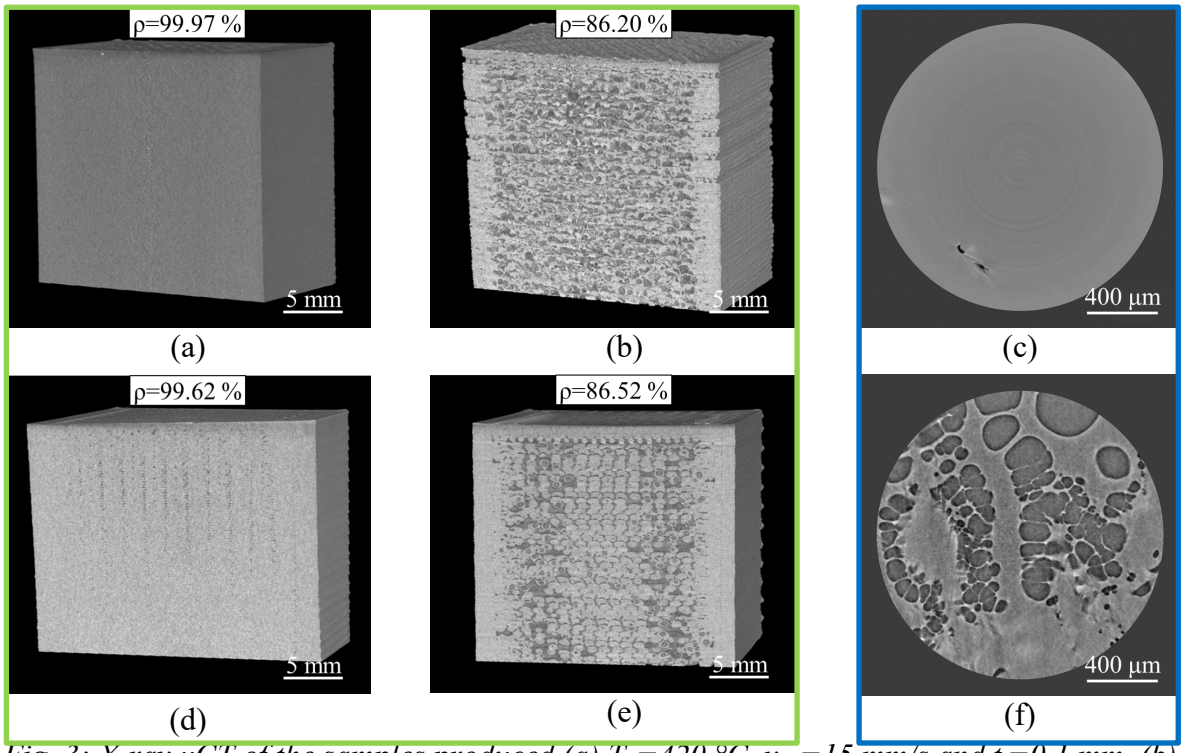

Fig. 3: X-ray µCT of the samples produced (a) T_n=420 °C, v_{nb}=15 mm/s and t_l=0.1 mm, (b) T_n=420 °C, v_{nb}=65 mm/s and t_l=0.2 mm, (d) T_n=380 °C, v_{nb}=15 mm/s and t_l=0.1 mm, (e) T_n=380 °C, v_{nb}=65 mm/s and t_l=0.2 mm, and Synchrotron X-ray µCT of the samples produced at (c) T_n=420 °C, v_{nb}=15 mm/s and t_l=0.1 mm, (f) T_n=420 °C, v_{nb}=65 mm/s and t_l=0.2 mm.

Chemical properties. No contaminants were found by EDSX inspections, while statistical analysis of the data showed that none of the investigated process parameters significantly influenced the carbon-oxygen weight ratio, which on average was C/O=3.57.

Ultra-High Vacuum behavior. The UHV behavior of the sample produced at T_n=380°C, v_n=15 mm/s and t_l=0.1 mm is shown in Fig. 4. No significant deviations from the background mass spectrum after bake-out at 120 °C were found, except for a small increase in O_2 and H_2, and a further reduction in partial pressure throughout the spectrum was obtained after bake-out at 200 °C. Therefore, it can be inferred that good levels of UHV can be achieved within a short time frame already at low bake-out temperature. This confirmed the suitability of PEEK for UHV applications as no significant outgassing level was recorded.

Materials Research Proceedings 35 (2023) 182-190 https://doi.org/10.21741/9781644902714-22

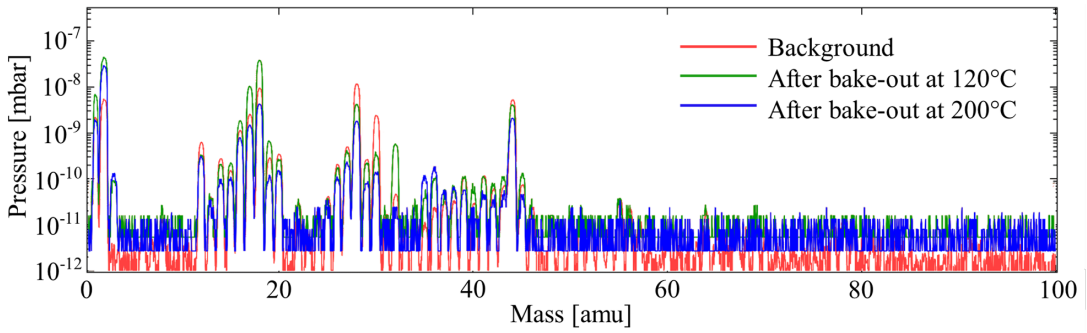

Fig. 4: Residual Gas Analysis under Ultra-High Vacuum condition of the samples produced at T_n =380 °C, v_{nb}=15 mm/s and t_l=0.1 mm.

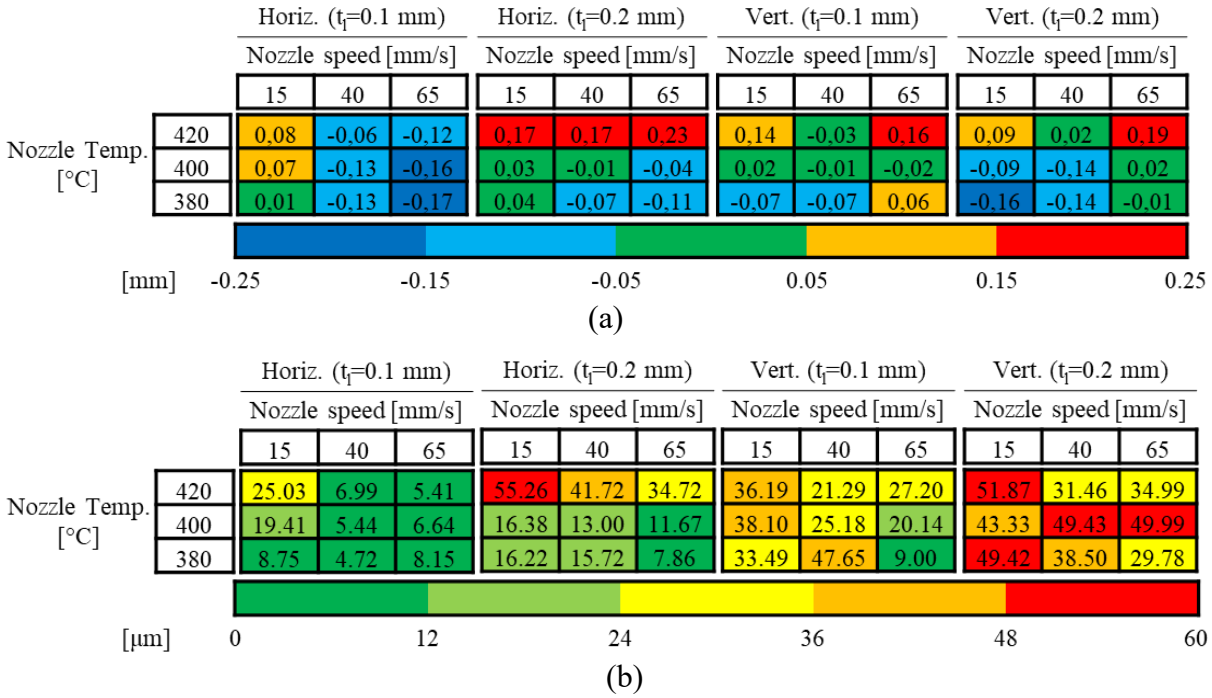

Fig. 5: Process maps obtained by analyzing the variability range of (a) the dimensional error and (b) the average surface roughness.

Optimal process parameters. Fig. 5 shows the process map obtained by classifying the dimensional errors and the average surface roughness according to Sturges' formula [13]. The optimal process conditions for each corresponding property are highlighted in dark green. The samples produced at T_n=380 °C, v_{nb}=15 mm/s and t_l=0.1 mm achieved the highest relative evaluation (two first-class ratings, one second-class rating, and one third-class rating). This set of parameters proved the capacity of providing the best surface quality, high hardness, and suitable parts for UHV applications, but they caused the formation of some under-extrusion pores. Other five sets of parameters achieved the same rating. However, three of them involved a high v_n, which proved to be unsuitable for producing dense and resistant parts. The remaining two sets involve intermediate v_n. These parameter sets would increase productivity, but additional tests are required to punctually examine the process output in this v_n range.

Overall, advanced optimization algorithms can be used to process this data from time to time to identify the optimal process parameters for specific multi-objective requirements. When doing this, productivity should also be considered.

Summary
In this paper, the influence of the nozzle temperature, nozzle speed and layer thickness on the properties of polyether ether ketone processed by Fused Deposition Modeling were analyzed with the aim of identifying the optimal process parameters. Results showed that geometrical conformity and surface quality can be generally improved by decreasing T_n and t_l, and by increasing v_n. However, highly porous material is obtained at high v_n and t_l either due to under-extrusion (low T_n) or due to flow and solidification phenomena (high T_n) resulting in complex structure of regularly-shaped pores. It was observed that the mechanical properties of the samples were primarily influenced by the material density, but even in fully dense conditions they were slightly lower compared to conventional material. Fully dense PEEK was instead proved to be suitable for UHV applications. However, further investigation in the intermediate v_n range is necessary to determine the absolute optimal process conditions.

Acknowledgements
The authors are grateful to Dott. D. Dreossi for performing μCT analysis, to Dott. L. Novinec for performing UVH tests and to Ing. I. Cudin for the helpful support. Part of the experimental work has been performed using the equipment acquired through the Croatian Science Foundation project IP-2019-04-3607 and by University of Rijeka under project uniri-tehnic-18-34. Elettra-Sincrotrone Trieste and the Laboratory for Advanced Mechatronics - LAMA FVG - of the University of Udine are also gratefully acknowledged for providing the equipment used for the experimental work and for the technical support. Emanuele Vaglio is grateful for funding under the REACT EU Italian PON 2014–2020 Program – Action IV.4 – Innovation (DM 1062, 10/08/2021).

References

[1] S.M. Kurtz, PEEK biomaterials handbook, second ed., William Andrew Publishing, 2019.

[2] R. Dua, Z. Rashad, J. Spears, G. Dunn and M. Maxwell, Applications of 3d-printed peek via fused filament fabrication: A systematic review, Polymers 13 (2021) 4046. https://doi.org/10.3390/polym13224046

[3] S. Ding, B. Zou, P. Wang and H. Ding, Effects of nozzle temperature and building orientation on mechanical properties and microstructure of PEEK and PEI printed by 3D-FDM, Polym. Test. 78 (2019) 105948. https://doi.org/10.1016/j.polymertesting.2019.105948

[4] P. Sikder, B.T. Challa and S.K. Gummadi, A comprehensive analysis on the processing-structure-property relationships of FDM-based 3-D printed polyetheretherketone (PEEK) structures, Materialia 22 (2022) 101427. https://doi.org/10.1016/j.mtla.2022.101427

[5] W. Wu, P. Geng, G. Li, D. Zhao, H. Zhang, and j. Zhao, Influence of layer thickness and raster angle on the mechanical properties of 3D-printed PEEK and a comparative mechanical study between PEEK and ABS, Materials 8 (2015) 5834-5846. https://doi.org/10.3390/ma8095271

[6] M. Vaezi and S. Yang, Extrusion-based additive manufacturing of PEEK for biomedical applications, Virtual Phys. Prototyp. 10 (2015) 123-135. https://doi.org/10.1080/17452759.2015.1097053

[7] A. Lee, M. Wynn, L. Quigley, M. Salviato and N. Zobeiry, Effect of temperature history during additive manufacturing on crystalline morphology of PEEK, Adv. Ind. Manuf. Eng. 4 (2022) 100085. https://doi.org/10.1016/j.aime.2022.100085

[8] C. Yang, X. Tian, D. Li, Y. Cao, F. Zhao and C. Shi, Influence of thermal processing conditions in 3D printing on the crystallinity and mechanical properties of PEEK material, J. Mater. Process. Technol. 248 (2017) 1-7. https://doi.org/10.1016/j.jmatprotec.2017.04.027

[9] A. El Magri, K. El Mabrouk, S. Vaudreuil, H. Chibane and M.E. Touhami, Optimization of printing parameters for improvement of mechanical and thermal performances of 3D printed poly (ether ether ketone) parts, J. Appl. Polym. Sci. 137 (2020) 49087. https://doi.org/10.1002/app.49087

[10] F. Zhao, D. Li and Z. Jin, Preliminary investigation of poly-ether-ether-ketone based on fused deposition modeling for medical applications, Materials 11 (2018) 288. https://doi.org/10.3390/ma11020288

[11] K. Okumura, Y. Tanaka and K. Iwai, Effect of Viscosity and Surface Roughness on Improvement of Solid-liquid Wettability by Ultrasonic Vibration, ISIJ Int. 62 (2022) 2217-2224. https://doi.org/10.2355/isijinternational.ISIJINT-2022-268

[12] E.A. Papon, A. Haque and S.B. Mulani, Process optimization and stochastic modeling of void contents and mechanical properties in additively manufactured composites, Compos. B: Eng. 177 (2019) 107325. https://doi.org/10.1016/j.compositesb.2019.107325

[13] H.A. Sturges, The choice of a class interval, J. Am. Stat. Assoc. 21 (1926) 65-66. https://doi.org/10.1080/01621459.1926.10502161